Int. J. Heat Mass Transfer. Vol. 32, No. 10, pp. 1821–1833, 1989
Printed in Great Britain

0017–9310/89 $3.00 + 0.00
Pergamon Press plc

Bubble number density and vapor generation in flashing flow

JOVICA R. RIZNIC
The Boris Kidric Institute of Nuclear Sciences, P.O. Box 522, Belgrade 11001, Yugoslavia

and

MAMORU ISHII†
School of Nuclear Engineering, Purdue University, West Lafayette, IN 47907, U.S.A.

(*Received* 26 *January* 1988 *and in final form* 25 *January* 1989)

Abstract—A phenomenon of flashing related to discharging initially subcooled liquid from a high pressure containment into a low pressure environment is very important in several industrial systems such as nuclear reactors and chemical reactors. A new model for the flashing process is proposed here based on the wall nucleation theory, bubble growth model and drift-flux bubble transport model. In order to calculate the bubble number density, the bubble number transport equation with a distributed source from the wall nucleation sites is used. The model predictions in terms of the void fraction are compared with Moby Dick and BNL experimental data. This result indicates that, at least for the experimental conditions considered here, the mechanistic prediction of the flashing phenomenon is possible, based on the present wall nucleation model.

1. INTRODUCTION

A PROBLEM of discharging an initially subcooled liquid from a high pressure condition into a low pressure environment is quite important in safety analyses of nuclear power, chemical and process plants. The dynamics of discharge and critical flow phenomena for single-phase fluids are well understood and acceptable analytical models are available. A number of problems arise for situations in which two-phase flow is involved. This is because the mechanical and thermal non-equilibrium effects as a consequence of liquid flashing may play an important role in the process.

In predicting two-phase flow transients, the interfacial transfer terms are among the most essential factors in modeling. These interfacial transfer terms in two-fluid models specify the rate of phase change, momentum exchange and heat transfer at the interface between phases. In the two-fluid model formulation [1–4], the transport processes of each phase are expressed by their own balance equations. Therefore, it is expected that the model can predict more detailed changes and phase interactions than a mixture model such as the drift-flux model [5, 6].

However, the weakest links in the two-fluid model are the constitutive equations for the interfacial interaction terms. The difficulties arise due to the complicated motion and geometry of the interfaces in a general two-phase flow. The interfacial transfer terms are strongly related to the interfacial area and to the local driving mechanisms, such as the degree of turbulence near the interfaces [1]. Basically, the interfacial transport of mass, momentum and energy is proportional to the interfacial area concentration and to a driving force. This area concentration defined as the interfacial area per unit volume of mixture, characterizes the kinematic effects; therefore, it must be related to the structure of the two-phase flow field. On the other hand, the driving forces for the interphase transport characterize the local transport mechanism, and they must be modeled separately. Basic macroscopic parameters related to the structure of two-phase flows, particularly of a dispersed (bubbly or droplet) flow, are the void fraction, particle number density, interfacial area concentration and the particle shape factor. From geometric considerations it is demonstrated that the particle number density is a key parameter in determining the interfacial area concentration but it has not been sufficiently investigated in the literature [7].

Realizing the significance of the bubble number density as an important parameter for predicting the interfacial area in a two-phase flow a model for the flashing process is proposed here based on the wall nucleation theory and the bubble growth model. In order to calculate the bubble number density, the bubble number transport equation is used.

2. FLASHING PHENOMENA

Flashing can be considered as a continuous process which occurs in several stages. Generally speaking,

† Author to whom correspondence should be addressed.

NOMENCLATURE

A_c cross-sectional area
Av Avogadro's number
B frequency of interaction of a molecule with its neighbors ($\approx kT$/Planck's constant)
C_0 distribution parameter
D_d bubble departure diameter
f bubble generation frequency
G mass velocity
g gravity
h interfacial heat transfer coefficient
h_{fg} latent heat of vaporization
J frequency of nucleation events per unit volume
j volumetric flux
Ja_p flashing Jakob number based on depressurization superheat
Ja_T Jakob number based on initial superheat
K_s sphericity correction factor
k Boltzmann constant
k_f thermal conductivity of liquid
m mass of the molecule
$\dot{N}$ rate of production of vapor nuclei
N_a active nucleation site density at wall
N_b bubble number density
N_h number of heterogeneous nucleation sites
N^* dimensionless active nucleation site density
$\hat{n}$ unit vector normal to the channel wall directed away from the fluid
$\hat{n}_\xi$ unit vector normal to ξ located in the cross-sectional plane and directed away from the fluid
R_b bubble radius
R_c critical cavity size
R_0 initial bubble radius
R_c^* dimensionless critical cavity radius, $R_c/(D_d/2)$
T temperature
T_f bulk fluid temperature
T_{sat} saturation temperature
T_w wall temperature
ΔT_{sup} wall superheat, $T_w - T_{sat}$
$\Delta T_{sup,f}$ effective superheat for nucleation under flashing
$\Delta T_{sup,sc}$ effective superheat for nucleation under normal or subcooled boiling
t time
V_{gj} drift-flux velocity
v volume
$\mathbf{v}_b$ local bubble velocity
$\bar{v}_b$ mean bubble velocity
v_r bubble relative velocity
$\mathbf{v}_\xi$ channel wall velocity
W_{cr} critical work required to create an unstable bubble nucleus
z axial coordinate
z_{eb} axial coordinate at point of flashing incipient
z_{C_0} axial coordinate at point where C_0 reaches 1.0.

Greek symbols

α void fraction
α_f thermal diffusivity of liquid
Γ_g vapor mass source rate
θ contact angle
ξ wetted (or heated) perimeter
ρ density
ρ^* non-dimensional density difference, $\Delta\rho/\rho_g$
$\Delta\rho$ density difference between liquid and vapor
σ surface tension between liquid and vapor
ϕ heterogeneity correction factor for critical work for bubble nucleation
ϕ_{he} heterogeneous bulk liquid nucleation rate
ϕ_{ho} homogeneous bulk liquid nucleation rate
ϕ_{si} bulk sink rate due to recondensation
ϕ_{so} bubble source rate due to bulk liquid nucleation
ϕ_w bubble nucleation rate from active cavities
Ω time constant for pressure variation.

Subscripts

b bubble
eb ebullition
f liquid phase
g vapor phase
he heterogeneous
ho homogeneous
w wall.

Superscript

* dimensionless quantities.

Averages

$\langle\langle\ \rangle\rangle$ area average
$\langle\ \rangle$ line average.

flashing occurs when liquid is brought to the region where the local pressure is below the saturation pressure corresponding to the liquid temperature. In a flowing system, such as the flow in a pipe or in a nozzle, a depressurization is caused by the friction or acceleration pressure drop which brings the liquid from initially subcooled to saturated conditions. With further decreases in the pressure, liquid becomes superheated and the nucleation process starts. The degree of superheat required for starting of the nucleation may depend on the flow and surface conditions for a particular flow system and the depressurization rate. For a pipe flow, in the beginning the bubble nucleation process is certainly dominated by wall heterogeneous nucleation. The process may be initially relatively slow, but it rapidly increases with increasing liquid superheat. According to Reocreux's experiments [8], this wall dominated vaporization zone was 20–120 cm in length. With relatively low liquid velocities in Reocreux's experiments, the characteristic time for generated vapor bubbles in this zone was of the order of a few tens of milliseconds. The length of the nucleation zone is a strong function of the flow velocity and the depressurization rate. For the BNL nozzle experiment [9] with similar pressure and temperature conditions as in Reocreux's experiment, the length of the nucleation zone was of the order of 1 cm only. This resulted from the higher flow velocities, depressurization rates and liquid superheating. A reliable predictive method is not yet established for the width of the bubble nucleation zone in a flowing flashing system, nor are exact criteria proposed for the point of flashing inception.

After the inception point, a local fluid pressure in a pipe decreases rapidly resulting in almost exponential increases of the liquid superheat. All vapor bubbles generated in the nucleation zone flowing through this region of the channel will experience sharp drops in pressure resulting in explosive bubble growth. Jones and Zuber [10] have found that for the variable pressure field where the pressure decays with time according to a power law t^n, the bubble radius varies as $t^{n+1/2}$ while the void fraction changes as $t^{3(n+1/2)}$. These very fast growing bubbles are accelerated more rapidly than the liquid phase. Thus after a short period of time the concentration profile becomes flatter, with C_0 approaching unity. Besides the flashing inception point, it is considered that this 'turning point' with $C_0 = 1.0$ is equally important for the thermo-hydraulics of the flashing, because it indicates the full migration of the bubbles to the core of the flow and sufficiently developed bubble profile. Vapor bubbles generated up to this turning point represent the majority of the bubble population which controls the vapor generation rate downstream in the channel. Bubbles generated downstream will have shorter growth time and much narrower changes in the pressure field, thus resulting in a lower partial void fraction. Saha *et al.* [11] in their model for vapor generation in flashing flow through nozzles, chose the inception point as the channel location after which the downstream nucleation can be neglected.

Further downstream, bubbles continue to expand and accelerate with a tendency to agglomerate into slug bubbles and into a continuous vapor core toward the annular flow regime. The development of those regimes in flashing flow depends on many parameters, including the pressure, flow rate, depressurization rate, surface conditions, presence of dissolved gases or impurities and local surface irregularities which may serve as nucleation and/or cavitation sites.

3. SOME PREVIOUS WORK

In recent years, the problem of flashing flow has often been studied in relation to the critical flow problem. Various models applicable to flashing with critical flow have been proposed in the past. Reviews and descriptions of these models have been presented by Ardron and Furness [12], Jones and Saha [13, 14], Weisman and Tentner [15], Abdollahian *et al.* [16] and D'Auria and Vigni [17].

Alamgir and Lienhard [18] developed a semi-empirical correlation to predict the pressure undershoot at the flashing inception point for a rapid static decompression of hot water. Jones [19] used their correlation and introduced a turbulence effect at the flashing onset point. Then he correlated Reocreux's [8] and Seynhaeve *et al.*'s [20] data for straight pipes. Reocreux [8] used a criterion for the flashing inception based on the superheat at the location where the pressure deviates from a linear axial profile. Our calculations [21] show that for Reocreux's experiments this inception point falls in the region where the local void fraction varies between 0.04 and 0.06. For these conditions, the generated vapor phase is still distributed in the vicinity of the wall and the distribution parameter C_0 is much lower than 1. This indicates that the void distribution profile is qualitatively similar to the one for subcooled boiling [6].

Edwards [22] assumed that the vapor phase is always at saturation and that Plesset and Zwick's [23] model could be applied for bubble growth in the initial phase of the flashing. Two arbitrary parameters, namely, the time-delay in bubble nucleation and the number of bubbles per unit mass of liquid were correlated using the data of Fauske [24] and Zaloudek [25]. The time-delay was of the order of 1 ms, and the bubble numbers calculated by Edwards were between 10^8 and 10^{11} bubbles lb^{-1}, i.e. about 2×10^5–2×10^8 bubbles cm^{-3}.

Malnes [26] assumed that the presence of dissolved gases has an important role in the flashing. He also made the assumption of a constant number of bubbles per unit volume which is a function of a property group

$$N_b = \left(\text{const.} \times g \frac{\rho_f}{\sigma} \right). \quad (1)$$

Instead of making this assumption about a constant number of bubbles, Rohatgi and Reshotko [27] used a kinetic theory and proposed an expression for the rate of production of vapor nuclei as

$$\dot{N} = N_h \frac{2\sigma}{\pi m} \exp\left[-\frac{W_{cr}}{kT_f}\phi\right] \quad (2)$$

where m, W_{cr} and k are the mass of the molecule, critical work required to create an unstable bubble nucleus and Boltzmann constant, respectively. In order to match Simoneau's experimental data [28], they recommended a value of $\phi = 5\times10^{-6}$ for the factor of heterogeneity and $N_h = 1$–2 nuclei cm^{-3} for the number of heterogeneous nucleation sites. Studovic [29] also used a kinetic theory approach to describe initial conditions for active nuclei vapor phase generation and modified Jones and Zuber's model [10] for the convex shape of the pressure distribution. He used his own experimental data from the converging–diverging nozzle, Reocreux's data [1] and data from the CANON experiment to correlate the vapor generation rate.

Following the theory of homogeneous nucleation, and using a liquid compression model, Lienhard and co-workers [30] proposed an expression for the bubble number density for a high pressure static decompression of water given by

$$N_b = \frac{\tilde{Z}}{(Ja_T + b\,Ja_p)^3} \quad (3)$$

where Ja_T and Ja_p represent the Jakob number based on initial superheat and a flashing Jakob number, respectively. The quantity $\tilde{Z}$ may be viewed as the bubble number density when an effective Jakob number, $Ja_T + b\,Ja_p$, has the value of unity. From various available experimental data they found that the mean value of 1.6×10^4 bubbles cm^{-3} describes the $\tilde{Z}$ data within 25% scatter. They assumed that the number density N_b remained constant during the flashing developments.

Wolfert [31] made an attempt to calculate the vapor generation, allowing relative movement between the vapor bubbles and the liquid. The effect of relative velocity has been incorporated in the interfacial heat transfer coefficient using Aleksandrov *et al.*'s expression [32] as

$$h = \frac{\sqrt{3k_f}}{\sqrt{(\pi\alpha_f t)}}\left[1+\sqrt{\left(\frac{2V_{gj}t}{3R_b}\right)}\right] \quad (4)$$

with the values of $V_{gj} = 0.15$ m s^{-1} and the number of bubbles $N = 5\times10^3$ bubbles cm^{-3}. Wolfert obtained the best agreement with Edwards and O'Brien's [33] standard experiment.

To predict the vapor distribution in the BNL nozzle experiments, Saha [34] provided a justification for Wolfert's model and proposed a modified expression for the interfacial heat transfer coefficient with the relative bubble velocity as

$$h = \frac{\sqrt{3k_f}}{\sqrt{(\pi\alpha_f t)}}\left[1+\frac{C_1}{3}\frac{V_{gj}t}{R_b}\right]^{1/2}. \quad (5)$$

A good agreement with the BNL flashing experiment data of Wu *et al.* [9] was obtained by best-fit calculations of the number of bubbles. For reported experiments, the number density of bubbles varies between 3×10^3 and 8×10^4 bubbles cm^{-3}.

In later papers, Jones and Shin [35, 36] proposed a wall cavity model to predict a flashing inception in the nozzles. Using Kocamustafaogullari and Ishii's [7] correlation for the site density, they attempted to find the bubble number density and the void at the nozzle throat (onset of flashing).

4. BUBBLE NUMBER TRANSPORT EQUATION

Kocamustafaogullari *et al.* [37] analyzed the problem of nucleation site density in pool and convective boiling, and developed a bubble number density balance equation. Following their procedure, the local bubble number density equation for flashing flow in a channel (Fig. 1) can be expressed as

$$\frac{\partial N_b}{\partial t} + \nabla(N_b \mathbf{v}_b) = \phi_{so} - \phi_{si} \quad (6)$$

where ϕ_{so}, ϕ_{si} and $\mathbf{v}_b$ are the bubble source term due to bulk nucleation, the bubble sink term due to bubble collapse or coalescence and the local bubble velocity, respectively.

For most engineering applications equation (6) can be simplified by means of proper averaging. The advantage of such an approach is two-fold. First, the variables appearing in the final equation will have explicit definitions in terms of averaged values. Consequently, it will be easy to compare predicted results with experimental data, which in two-phase flow are most often presented in terms of average values. Second, by means of space averages it will be possible to reduce the number of space variables and to treat the problem as a one-dimensional one.

In order to simplify equation (6) into a one-dimensional form and to express it by means of averaged values of the variables, let us integrate the local bubble number density balance equation over the channel cross-sectional area, $A_c(z)$. Thus

$$\iint_{A_c(z)} \frac{\partial N_b}{\partial t}\,dA + \iint_{A_c(z)} \nabla(N_b \mathbf{v}_b)\,dA = \iint_{A_c(z)} (\phi_{so} - \phi_{si})\,dA. \quad (7)$$

The first integral on the left-hand side is transformed by means of the Leibnitz theorem over surfaces as

$$\iint_{A_c(z)} \frac{\partial N_b}{\partial t}\,dA = \frac{\partial}{\partial t}\iint_{A_c(z)} N_b\,dA - \int_{\xi(z)} \frac{\hat{n}\cdot(N_b\mathbf{v}_\xi)}{(\hat{n}\cdot\hat{n}_\xi)}\,d\xi \quad (8)$$

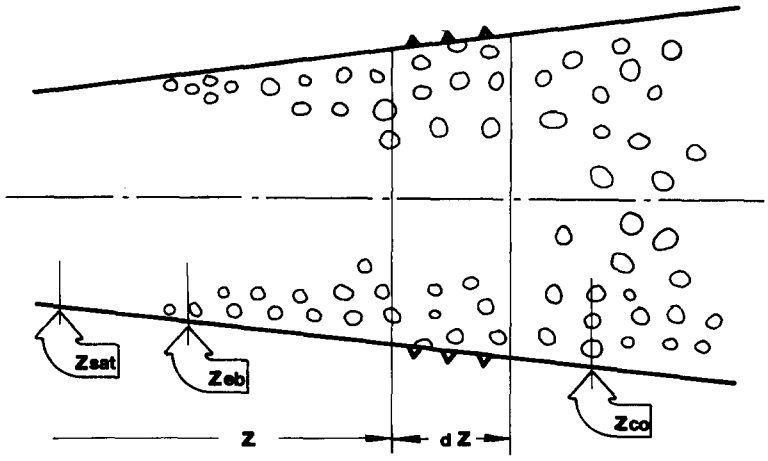

FIG. 1. A schematic representation of the channel bubble flow for flashing model.

whereas the second integral can be evaluated by means of the Gauss–Ostrogradskii divergence theorem over surfaces as

$$\iint_{A_c(z)} \nabla\cdot(N_b\mathbf{v}_b)\,dA = \frac{\partial}{\partial z}\iint_{A_c(z)} (N_b v_{bz})\,dA + \int_{\xi(z)} \frac{\hat{n}\cdot(N_b\mathbf{v}_b)}{(\hat{n}\cdot n_\xi)}\,d\xi. \quad (9)$$

Substituting equations (8) and (9) in equation (7) and then rearranging, we obtain

$$\frac{\partial}{\partial t}\iint_{A_c(z)} N_b\,dA + \frac{\partial}{\partial z}\iint_{A_c(z)} (N_b v_{bz})\,dA = -\int_{\xi(z)} \frac{\hat{n}\cdot N_b(\mathbf{v}_b-\mathbf{v}_\xi)}{(\hat{n}\cdot\hat{n}_\xi)}\,d\xi + \iint_{A_c(z)} (\phi_{so}-\phi_{si})\,dA \quad (10)$$

where $\xi(z)$ is the intersection of the channel wall with the cross-sectional plane, $\hat{n}$ the unit vector normal to the channel wall and $\hat{n}_\xi$ the unit vector normal to ξ. The usual expression for the area averaged value of any quantity F is given by

$$\langle\langle F\rangle\rangle(z,t) = \frac{1}{A_c(z)}\iint_{A_c(z)} F(x,y,z,t)\,dA. \quad (11)$$

The mean bubble velocity is defined by a weighted mean value given by

$$\bar{v}_b = \langle\langle N_b v_{bz}\rangle\rangle/\langle\langle N_b\rangle\rangle. \quad (12)$$

Equation (10) can be expressed in the following form:

$$\frac{\partial}{\partial t}(A_c\langle\langle N_b\rangle\rangle) + \frac{\partial}{\partial z}(A_c\langle\langle N_b\rangle\rangle\bar{v}_b) = -\int_{\xi(z)} \frac{\hat{n}N_b\cdot(\mathbf{v}_b-\mathbf{v}_\xi)}{(\hat{n}\cdot\hat{n}_\xi)}\,d\xi + A_c(\langle\langle\phi_{so}\rangle\rangle - \langle\langle\phi_{si}\rangle\rangle). \quad (13)$$

The first term on the right-hand side represents the flux of bubbles generated from the active nucleation sites at the channel wall. In terms of the bubble nucleation site density N_a and the frequency f of bubbles generated from a nucleation site, the bubble flux term can be given by

$$-\hat{n}\cdot N_b(\mathbf{v}_b-\mathbf{v}_\xi) = N_a f. \quad (14)$$

Substituting equation (14) into equation (13) one obtains

$$\frac{\partial}{\partial t}(A_c\langle\langle N_b\rangle\rangle) + \frac{\partial}{\partial z}(A_c\langle\langle N_b\rangle\rangle\bar{v}_b) = -\int_{\xi(z)} \frac{N_a f}{(\hat{n}\cdot\hat{n}_\xi)}\,d\xi + A_c(\langle\langle\phi_{so}\rangle\rangle - \langle\langle\phi_{si}\rangle\rangle). \quad (15)$$

Equation (15) is the one-dimensional, area-averaged bubble number density transport equation, which is applicable for a channel with a variable cross-sectional plane. For the case of flow in a pipe with a constant cross-sectional area, it can be simplified to the form

$$\frac{\partial\langle\langle N_b\rangle\rangle}{\partial t} + \frac{\partial}{\partial z}(\langle\langle N_b\rangle\rangle\bar{v}_b) = \langle\phi_w\rangle + \langle\langle\phi_{so}\rangle\rangle - \langle\langle\phi_{si}\rangle\rangle. \quad (16)$$

The perimeter-averaged bubble generation rate from active nucleation sites at the channel wall is given by

$$\langle\phi_w\rangle = \frac{1}{A_c}\int_\xi (N_a f)\,d\xi = \frac{\langle N_a\rangle f\xi}{A_c} \quad (17)$$

with the assumption that the frequency f is uniform around the channel perimeter.

Bubble nucleation in the bulk liquid can occur either as homogeneous or heterogeneous nucleation. The classical homogeneous nucleation theory assumes that a bubble is formed in the bulk liquid by the

vaporization of molecules of the liquid into a cavity. This cavity may be considered as any space within the liquid phase unoccupied by liquid molecules, thus it can be either empty or occupied by vapor. According to the Volmer–Döring–Zeldovich theory [38], the homogeneous nucleation rate can be expressed by

$$J_{ho} = \rho_f Av\, B \exp\left[-W_{cr}/kT\right] \tag{18}$$

where Av and B are Avogadro's number and frequency with which a molecule within the liquid interacts with its neighbors.

Foreign particles and dissolved gas normally provide ample nuclei to act as centers of vapor formation. The vapor generation from pre-existing nuclei in the liquid is usually called heterogeneous nucleation. The presence of particles and dissolved gas reduces the liquid superheat required to maintain a bubble in unstable equilibrium. The heterogeneous nucleation rate can be expressed in a similar form as

$$J_{he} = \rho_f Av\, B \exp\left[-W_{cr}\phi/kT\right] \tag{19}$$

where ϕ is the factor of heterogeneity. This factor modifies the critical work needed to create a cavity for a heterogeneous nucleation case. In the papers by Ward *et al.* [39] and Forest and Ward [40] it has been shown that the presence of dissolved gas can initiate nucleation even at temperatures below the saturation corresponding to the local liquid pressure. Unfortunately, for water all those theories yield extremely high liquid superheats, especially at lower pressure. As stated by Skripov [41], it is possible that for some reason the classical theory itself is not applicable to water at $P < 0.5\, p_{cr}$.

The third term on the right-hand side of equation (16), the sink term $\langle\langle \phi_{si} \rangle\rangle$, takes care of the reduction in bubble number density due to the coalescence of bubbles into larger bubbles or bubble collapse. The coalescence is assumed to be insignificant up to the void fraction α_{C_0} corresponding to the point with a reasonably homogeneous distribution of a vapor phase in the bulk liquid, i.e. the point where the distribution parameter C_0 reaches unity. For the flow conditions in the experiments of Reocreux [8] and BNL [9] the distribution parameter C_0 has a value of 1.0 for the void fraction α in the vicinity of 0.1 according to the drift-flux correlation [6]. Certainly this assumption can be extended up to the void fraction of 0.3 beyond which the flow regime transition to the slug or churn-turbulent flow occurs.

5. VAPOR GENERATION MODEL FORMULATION

For a steady-state flow equation (15) can be rewritten as

$$\frac{\partial}{\partial z}(A_c N_b v_b) = (\phi_w + \phi_{ho} + \phi_{he} - \phi_{si}) A_c. \tag{20}$$

Here ϕ_w, ϕ_{ho}, ϕ_{hi} and ϕ_{si} are the sources due to wall, homogeneous and bulk heterogeneous nucleations and the sink due to coalescence or collapse, respectively. Furthermore, various averaging symbols are omitted for simplicity. The sink term may be neglected for the beginning of a flashing flow, thus after an integration from z_{sat} to z, one obtains

$$A_c N_b(z) v_b(z) = \int_{z_{sat}}^{z} A_c(\phi_w + \phi_{ho} + \phi_{he})\, dz. \tag{21}$$

Here z_{sat} is the point at which the liquid reaches the saturation condition (see Fig. 1). Equation (21) can be solved for the bubble number densities at the flashing inception point $N_{b,z_{eb}}$ and the turning point $N_{b,z_{C_0}}$, respectively, i.e.

$$N_{b,z_{eb}} = \frac{1}{A_c v_{b,z_{eb}}} \int_{z_{sat}}^{z_{eb}} A_c(\phi_w + \phi_{ho} + \phi_{he})\, dz \tag{22}$$

$$N_{b,z_{C_0}} = \frac{1}{A_c v_{b,z_{C_0}}} \int_{z_{sat}}^{z_{C_0}} A_c(\phi_w + \phi_{ho} + \phi_{he})\, dz. \tag{23}$$

It is noted that at the turning point the distribution parameter C_0 reaches 1, thus a considerable number of bubbles migrated to the central part of a flow channel. The wall nucleation rate ϕ_w may be expressed by using the correlation developed by Kocamustafaogullari and Ishii [7, 37] for nucleation site density. They found that the wall nucleation site density can be correlated in dimensionless form as

$$N_{ns}^* = R_c^{*-4.4} f(\rho^*). \tag{24}$$

The non-dimensional site density is defined by

$$N_{ns}^* = N_{ns} D_d^2 \tag{25}$$

and the non-dimensional critical cavity radius by

$$R_c^* = \frac{R_c}{(D_d/2)} \quad \text{with} \quad R_c \simeq \frac{2\sigma T_{sat}}{(T_w - T_{sat})\rho_g h_{fg}} \tag{26}$$

where D_d is the bubble departure diameter. The property function is correlated in terms of the density ratio as

$$f(\rho^*) = 2.157 \times 10^{-7} \left(\frac{\Delta\rho}{\rho_g}\right)^{-3.12} \left(1 + 0.0049 \frac{\Delta\rho}{\rho_g}\right)^{4.13}. \tag{27}$$

Originally the correlation was developed for pool and convective boiling, and the data were correlated by using different effective superheat for those two types of boiling. Our calculations show that this correlation can be generalized even for the flashing flow by introducing the appropriate superheat in the boundary layer where the bubble is generated. For convective boiling, the effective liquid superheat to which the nucleation sites and growing bubbles at the wall are exposed fluctuates between $(T_w - T_{sat})$ and 0 due to the nucleation, evaporation and liquid convection. Therefore, in the sense of averaged values,

the mean superheat is of the order of $\Delta T_{sup,sc} \simeq \Delta T/2$. However, in the correlation development for the nucleation site density, the apparent superheat ΔT has been used. On the other hand, in flashing flow, the bulk liquid is superheated. Thus the effective superheat for nucleation is ΔT, because there is always sufficient supply of superheated liquid at the wall. The bubbles are initiated from smaller wall cavities and the bubbles grow much faster than in convective boiling. Thus it is postulated here that the active nucleation site density correlation obtained for the pool and forced convective boiling could be used to predict the active nucleation site density in flashing with an effective average superheat $\Delta T_{sup,f} = \Delta T_{sup}$ rather than $\Delta T_{sup,sc}$. Practically this will result in smaller critical radii of cavities. Thus the effective nucleation site density for flashing flow is given by modifying equation (24) as

$$N_{ns}^{*} = \frac{1}{(D_d/2)} \left\{ \frac{2\sigma T_{sat}}{2(T_f - T_{sat})\rho_g h_{fg}} \right\}^{-4.4} f(\rho^{*}). \quad (28)$$

Jones and Shin [35] reported the values for the minimum critical cavity sizes from their analytical wall cavity model. The present calculations, using the superheat $\Delta T_{sup,f}$, and the effective critical cavity size expression by Kocamustafaogullari and Ishii [37], are within a few percent of theirs. A bubble departure diameter D_d, necessary to obtain an active nucleation site density N_{ns} is determined by Kocamustafaogullari's model [42] given by

$$D_d = 2.64 \times 10^{-5} \theta \left(\frac{\sigma}{g\Delta\rho} \right)^{0.5} \left(\frac{\Delta\rho}{\rho_g} \right)^{0.9}. \quad (29)$$

To estimate the frequency of bubble departures the expression given by Zuber [43] is adopted here, thus

$$D_d f = 1.18 \left[\frac{\sigma g(\rho_f - \rho_g)}{\rho_f^2} \right]^{1/4}. \quad (30)$$

Using the expressions given by equations (17) and (25)–(30) one can find the bubble nucleation rate at the wall. Furthermore, by integrations given by equations (22) and (23) it is possible to determine the bubble number densities at the location of flashing inception and the turning point, i.e. where the distribution parameter C_0 has the value of ~ 1.0. Applying the bubble growth law in the variable pressure field [10] it is possible to estimate a bubble radius by

$$R(t) = \left(\frac{\rho_{g,0}}{\rho_g} \right)^{1/3} \left\{ R_0 + \frac{2K_s}{\sqrt{\pi}} Ja_T \sqrt{(\alpha_f t)} + \frac{2K_s}{\sqrt{\pi}} Ja_p \frac{\sqrt{\alpha_f}}{\Omega} [\sqrt{(\Omega t)} - D(\sqrt{(\Omega t)})] \right\} \quad (31)$$

where Ω and $D(\Omega t)$ represent time constants for pressure variation and the Dawson integral. With the idealization that all bubbles are spherical, the void fraction can be given by

$$\alpha(t) = N_b(z) \tfrac{4}{3}\pi R_b^3(t) \quad (32)$$

if the bubbles have the uniform size $R_b(t)$. However, in most applications bubble sizes are not uniform due to the differences in residence times. This effect is considered below.

At an early stage of the steady-state flashing process in a channel, the wall nucleation due to fluid superheat caused by the pressure drop controls the process. Thus in equation (20), the wall nucleation source, ϕ_w, dominates the term on the right-hand side. The sink term, ϕ_{si}, due to the bubble collapse or coalescence is basically zero in bulk superheated liquid and for very small bubbles which are in the early stages of bubble growth. The bulk homogeneous nucleation source ϕ_{ho} is negligible because the liquid superheat is relatively low. Thus the preferred site nucleation such as the wall nucleation should be much more significant than ϕ_{ho}. The bulk heterogeneous nucleation source ϕ_{he} can be significant only if a considerable amount of dissolved gas is present in the liquid. For the present study it is assumed that the effect of dissolved gas is negligible on the nucleation process.

From the above considerations, the bubble number transport equation becomes

$$\frac{\partial}{\partial z}(A_c N_b v_b) \simeq A_c \phi_w. \quad (33)$$

By integration from the boiling initiation point, z_{sat}, to z_1, one obtains

$$N_b(z_1) = \frac{1}{A_c(z_1) v_b(z_1)} \int_{z_{sat}}^{z_1} \phi_w A_c \, dz. \quad (34)$$

Here the number density $N_b(z_1)$ includes the contributions from all the bubbles nucleated upstream of point z_1.

The local contribution can be considered by introducing a new parameter $n_b(z_1, z)$ which is defined by

$$n_b(z_1, z) = \frac{\phi_w(z) A_c(z)}{A_c(z_1) v_b(z_1)}. \quad (35)$$

This parameter represents the contribution from the nucleation sites at location z, i.e. a number of bubbles per unit length of a channel originating at z and arriving at z_1.

Using the Lagrangian description, the void fraction at z can be given by

$$\alpha(z_1) = \int_{z_{sat}}^{z_1} \tfrac{4}{3}\pi R^3(t(z)) n_b(z_1, z) \, dz. \quad (36)$$

The time scale following the bubble can be calculated by integrating the relation

$$dz = v_b(z) \, dt. \quad (37)$$

For simplicity, all the bubbles within a cross section are assumed to be flowing with the average velocity $v_b(z)$. Then

$$t = \int_{z}^{z_1} \frac{dz}{v_b(z)}. \quad (38)$$

In the above formulation the bubble average velocity v_b is unknown. The expression for v_b can be obtained from the continuity relations. The vapor continuity equation is given [1, 6] by

$$\frac{\partial}{\partial t}(A_c \alpha \rho_g) + \frac{\partial}{\partial z}(A_c \alpha \rho_g v_b) = \Gamma_g A_c \quad (39)$$

where Γ_g is the vapor mass source term. On the other hand, the volumetric flux equation is given by

$$\frac{\partial}{\partial z}(A_c j) = \Gamma_g A_c \left(\frac{\Delta \rho}{\rho_g \rho_f}\right). \quad (40)$$

Here j is given by $j = \alpha v_b + (1-\alpha)v_f$. Under a steady-state condition, Γ_g can be eliminated between equations (39) and (40) after integrations to yield

$$\frac{\alpha \rho_g v_b}{j - v_{fi} A_c(z_{sat})/A_c} = \frac{\rho_g \rho_f}{\Delta \rho} \quad (41)$$

where v_{fi} is the liquid velocity at the boiling initiation point $z = z_{sat}$.

Furthermore, the relative velocity correlation can be given by the drift flux formulation [6]. In terms of the vapor velocity and the total volumetric flux, it is given by

$$v_b = C_0 j + \langle\langle V_{gj} \rangle\rangle. \quad (42)$$

Here C_0 is the distribution parameter which accounts for the slip due to phase and velocity distributions, and $\langle\langle V_{gj} \rangle\rangle$ is the averaged local drift velocity for the local slip between phases. Both C_0 and $\langle\langle V_{gj} \rangle\rangle$ should be expressed by a constitutive relation. For the region near the boiling initiation point, Ishii [6] recommends

$$C_0 = (1.2 - 0.2\sqrt{(\rho_g/\rho_f)})(1 - e^{-18\alpha}). \quad (43)$$

It is noted that this expression has been obtained for a standard boiling flow in a heated pipe and not particularly for a flashing flow. Since the boiling processes are different, the exponent in equation (43) can differ from the one given there. However, the trend indicated by equation (43) is correct for a flashing flow also, thus as a first approximation, equation (43) is used here. For a vertical churn-turbulent bubbly flow, the local drift velocity is given by

$$\langle\langle V_{gj} \rangle\rangle = \sqrt{2}\left(\frac{\sigma g \Delta \rho}{\rho_f^2}\right)^{1/4}. \quad (44)$$

However, the local drift velocity strongly depends on two-phase flow regimes and flow direction, thus a careful treatment of this term is necessary [6].

Equations (41) and (42) give the expression for v_b in terms of the void fraction, since the total volumetric flux can be eliminated between the two equations. Thus by using the bubble growth model such as equation (31), the solution for the void fraction can be obtained from equation (36) with equations (38), (41) and (42). The above formulation is used to calculate the void fraction in the region where the wall nucleation effect is important.

However, at a certain point the effect of the new wall nucleations on the void fraction become rapidly insignificant in the downstream section because of the increased number density and a relatively large average bubble size. In this bubble expansion region, some simplication can be made by setting the bubble source term ϕ_w to zero. In the present analysis it has been assumed that downstream of the location in the channel where the distribution parameter C_0 reaches unity the contribution of the newly generated bubbles from wall nucleation may be neglected for the void fraction calculation.

The bubble growth within a flow field is larger than the one for a stationary case. An approximate theoretical result to account for the relative velocity effect on the bubble growth has been obtained by Aleksandrov *et al.* [32]. This can be given as a modification to the stationary case in the following form:

$$\left(\frac{dR_b}{dt}\right)_{v_r \neq 0} = \left(\frac{dR_b}{dt}\right)_{v_r = 0}\left[1 + \frac{2}{3}\frac{v_r t}{R_b}\right]^{1/2} \quad (45)$$

where the case with $v_r = 0$ denotes the stationary bubble growth rate. This can be given, for example, by the Jones–Zuber [10] model, equation (26) for a stationary bubble.

The result of Aleksandrov *et al.* [32] has been applied by several researchers to study bubble growth rates in flowing systems. In order to use the above result the local relative velocity should be specified. Florschuetz *et al.* [46] and Wolfert [31] assumed a linear relation between the relative velocity and the bubble radius, thus

$$v_r = \text{const.} \times R_b. \quad (46)$$

On the other hand, Saha [34] used a local bubble drift velocity $\langle\langle V_{gj} \rangle\rangle$. For relatively slow processes of depressurization of flow in a pipe or a nozzle, the average local drift velocity $\langle\langle V_{gj} \rangle\rangle$ may be assumed to be constant for relatively large bubbles. However, it is also possible to use more complicated correlations based on the drift-flux model [6]. The average local relative velocity can be given approximately by

$$v_r = \frac{\langle\langle V_{gj} \rangle\rangle}{1-\alpha} \quad (47)$$

which can be used in equation (45) together with the correlation for the drift velocity.

6. COMPARISONS WITH THE EXPERIMENTS

A computer program ULYSSYS was developed to solve the equations of the model. The system of equations is solved by using the bubble number density, the void fraction and the bubble growth equations (31) and (34)–(36), together with the nucleation site density expressions (24)–(27), and bubble relative

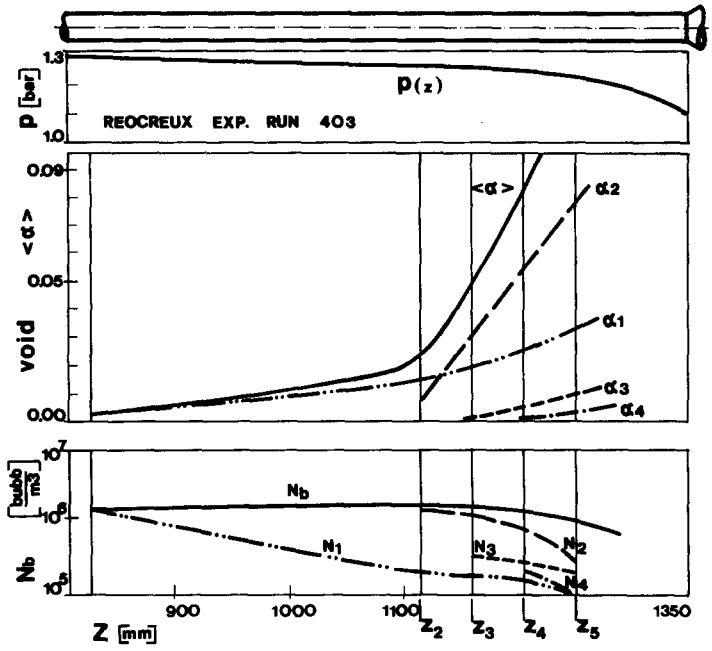

FIG. 2. Bubble number density distribution along Reocreux's test channel.

velocity (47). These are supplemented by the specified system geometry and necessary properties. The time is eliminated by a simple time–space coordinate transformation using the vapor velocity. The result is a set of three algebraic equations for α, N_b and R_b which can be solved successively by standard numerical techniques. The present model has been applied to steady-state flashing experiments conducted in vertical channels. In the present study, an attempt was made to compare the model predictions with the experimental data of Reocreux [8] and BNL [9]. The test channel [8] was made in two parts. The lower part consisted of a stainless steel tube with an internal diameter of 20 mm and with a length of 2160 mm. The upper part made up the test channel proper. It consisted of a cylindrical part with an internal diameter of 20 mm followed by a divergent section with a peak angle of 7° and a length of 327 mm and a last cylindrical part with a diameter of 60 mm. Initially subcooled water at low pressures (0.21–0.34 MPa) entered the test section at the bottom and flowed upwards. As the pressure decreased, flashing began and two-phase mixture flowed through the cylindrical and the diverging part of the channel. Pressure and area-averaged void fractions were measured along the length of the test section. The accuracy of the pressure measurement was within 1% of the reading and that for the void fraction was within 0.05. The accuracy for the fluid temperature measurement was within 0.1°C [11].

Some results of the present model predictions of bubble number density distribution along Reocreux's channel for run 403 are shown in Fig. 2 [44]. It can be noticed that the main contribution of void coming from the bubbles generated in the section between z_{sat} and net vapor generation location. The contribution of bubbles generated downstream is much smaller, due to the differences in residence time.

The above model formulation is used to calculate the void fraction in the region where the wall nucleation effect is important. However, at a certain point the effect of the new wall nucleations on the void fraction becomes rapidly insignificant in the downstream section because of the increased number density and a relatively large average bubble size. In this bubble expansion region, some simplification can be made by setting the bubble source term ϕ_w to zero. In the present analysis it has been assumed that downstream of the location in the channel where the distribution parameter C_0 reaches unity the contribution of the newly generated bubbles from wall nucleation may be neglected. For the void fraction calculation the results of the comparisons between the present model predictions and Reocreux's few experimental trials are given in Figs. 3–7. The model predictions are in fairly good agreement with Reocreux's data up to the critical flow plane (throat) in his test channel. Downstream of the throat (z_{C_0} = 1351 mm) the model predicts voids lower than experimental values. One of the reasons is probably the presence of secondary flows in the vicinity of the throat. Reocreux reported [8] that the radial distribution of the void in the diverging zone indicates that the two-phase mixture does not expand completely. The same phenomenon was observed in the experiments with visualization using the glass test channel. In the same figure are also shown results from the model with the assumption that the two-phase jet leaves the throat without any expansion, and that the space between

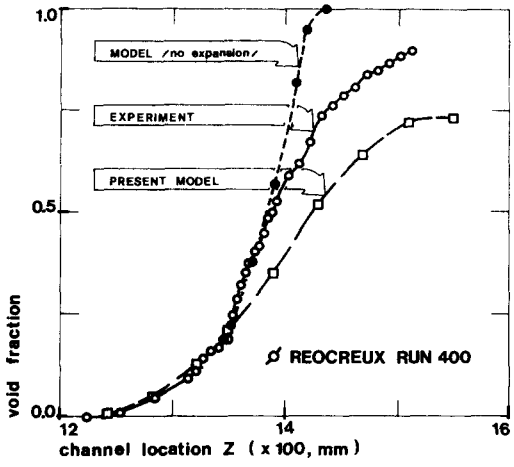

FIG. 3. Comparison between the present model prediction and Reocreux's experimental trial 400.

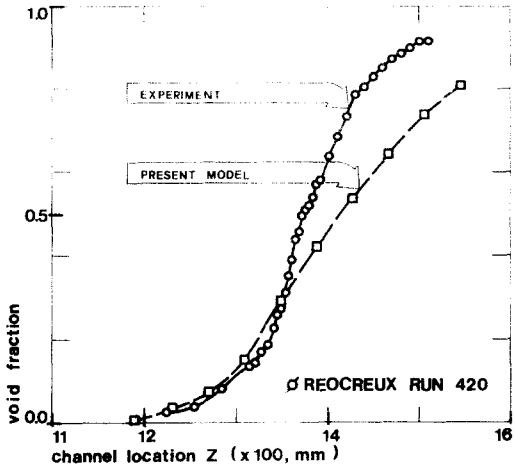

FIG. 6. Comparison between the present model prediction and Reocreux's experimental trial 420.

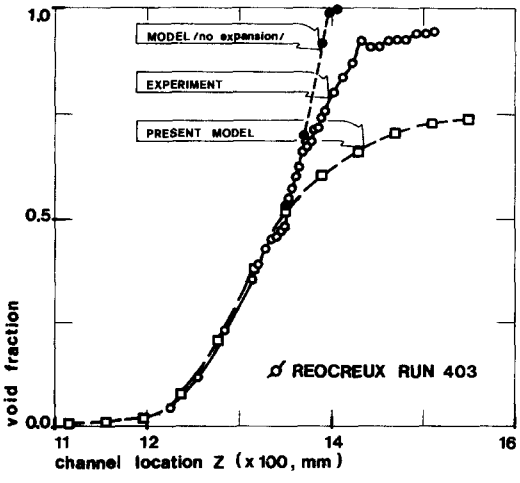

FIG. 4. Comparison between the present model prediction and Reocreux's experimental trial 403.

the jet and channel wall is filled with vapor phase. It can be seen from those figures that the calculated void profile is very close to the experimentally observed one up to the characteristic length of $(2 \sim 3)\ D_{\text{tube}}$ from the throat.

Experimental data for BNL nozzle run 137 are given in Fig. 8. Because of much higher velocities than in Reocreux's case, the presence of roll waves immediately after the throat (314.8 mm) have even more influence on the void distribution in the diverging part of the channel.

Comparisons of the model with the data show that the model based on the nucleation site density correlation appears to be acceptable to describe vapor generation in the flashing flow. For the limited data examined here, the comparisons show rather satisfactory agreement without using a floating parameter to adjust the model.

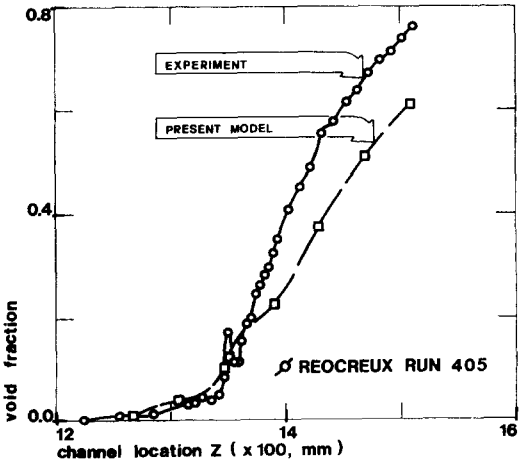

FIG. 5. Comparison between the present model prediction and Reocreux's experimental trial 405.

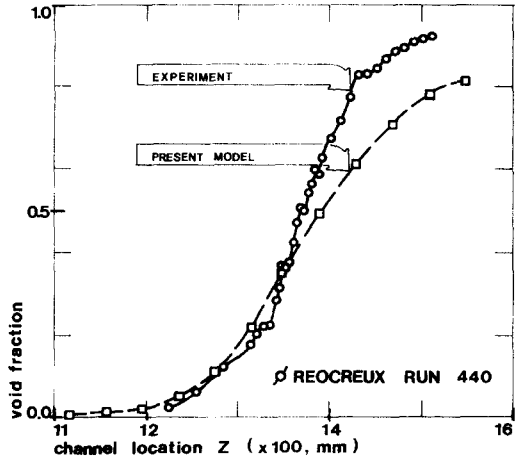

FIG. 7. Comparison between the present model prediction and Reocreux's experimental trial 440.

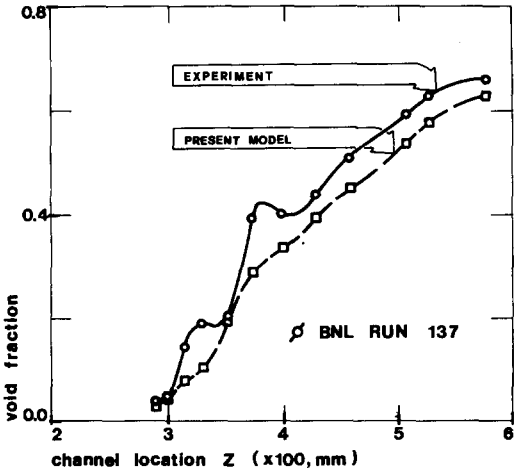

FIG. 8. Comparison between the present model prediction and BNL experimental run 137.

7. CONCLUSIONS

A new model for flashing flow based on wall nucleations is proposed here and model predictions are compared with some experimental data. The bubble number density and volumetric flux transport equations are used. Thus it was possible to avoid the usually made assumption with constant bubble number density. Also, a vapor generation rate equation is derived. A correlation for the nucleation site density is adopted for application in the flashing flow. The model predictions compared with the experimental data of Reocreux and BNL showed that satisfactory agreement could be obtained with the present model without any floating parameter to adjust the data.

Acknowledgements—This work was performed while one of the authors (J. Riznic) was on leave at the Argonne National Laboratory, under the auspices of the International Atomic Energy Agency and the National Research Council of the U.S. National Academy of Sciences. A grant received from these institutions is deeply acknowledged. This work is partially funded by the U.S. Nuclear Regulatory Commission. The authors would like to express their appreciation to Drs N. Zuber and Richard Lee of NRC and Prof. G. Kocamustafaogullari of the University of Wisconsin at Milwaukee for valuable discussions on the subject.

REFERENCES

1. M. Ishii, *Thermo-fluid Dynamic Theory of Two-phase Flow*. Eyrolles, Paris (1975).
2. P. Vernier and J. M. Delhaye, General two-phase flow equations applied to the thermodynamics of boiling nuclear reactor, *Energ. Prim.* **4**(1), 5–46 (1968).
3. J. Boure and M. Reocreux, General equations of two-phase flows, *Proc. 4th All Union Heat Transfer Conf.*, Minsk, U.S.S.R. (1972).
4. G. Kocamustafaogullari, Thermo-fluid dynamics of separated two-phase flow, Ph.D. Thesis, School of Mechanical Engineering, Georgia Institute of Technology, Georgia (1971).
5. N. Zuber, Flow excursions and oscillations in boiling two-phase systems with heat addition, *Proc. EURATOM Symp. on Two-phase Dynamics*, Vol. 1, pp. 1070–1089. Commission of European Communities, Brussels (1967).
6. M. Ishii, One-dimensional drift-flux model and constitutive equations for relative motion between phases in various two-phase flow regimes, ANL-77-47, Argonne National Laboratory (1977).
7. G. Kocamustafaogullari and M. Ishii, Interfacial area and nucleation site density in boiling systems, *Int. J. Heat Mass Transfer* **26**, 1377–1387 (1983).
8. M. Reocreux, Contribution to the study of critical flow rates in two-phase water vapor flow, Ph.D. Thesis, Medical University of Grenoble (1974), NUREG-tr-0002 (1978).
9. B. J. C. Wu, N. Abuaf and P. Saha, A study of non-equilibrium flashing of water in a converging–diverging nozzle, NUREG/CR-1864, BNL-NUREG-51317 (June 1981).
10. O. C. Jones, Jr. and N. Zuber, Evaporation in variable pressure fields, Paper No. 76-CSME-CSCLE-12, Natl Heat Transfer Conf. (1976) and *Trans. ASME, J. Heat Transfer* **100C**, 453–459 (1978).
11. P. Saha, N. Abuaf and B. J. C. Wu, A non-equilibrium vapor generation model for flashing flows, paper presented at the 20th ASME/AIChE Natl Heat Transfer Conf., Milwaukee, Wisconsin, 2–5 August (1981). Also published in *J. Heat Transfer* **106**(1), 198–203 (February 1984).
12. K. H. Ardron and R. A. Furness, A study of the critical flow models used in reactor blowdown analysis, *Nucl. Engng Des.* **39**, 257–266 (1976).
13. O. C. Jones, Jr. and P. Saha, Non-equilibrium aspects of water reactor safety, *Proc. Symp. on the Thermal and Hydraulic Aspects of Nucl. Reactor Safety*, Vol. 1, *Light Water Reactors* (Edited by O. C. Jones, Jr. and S. G. Bankoff). ASME, New York (1977).
14. P. Saha, Review of two-phase steam–water critical flow models with emphasis on thermal non-equilibrium, NUREG/CR-0417, BNL-NUREG-50907 (1972).
15. J. Weismann and A. Tentner, Models for estimation of critical flow in two-phase systems, *Prog. Nucl. Energy* **2**, 183–197 (1978).
16. D. Abdollahian, J. Healzer and E. Janseen, Critical flow data review and analysis. Part I—literature survey, SL I-7908-1, revised 11/80 (November 1980).
17. F. D'Auria and P. Vigni, Two phase critical flow models, CSNI Report No. 49 (May 1980).
18. Md. Alamgir and J. H. Lienhard, Correlation of pressure undershoot during hot-water depressurization, *J. Heat Transfer, ASME* **103**(1), 52–55 (February 1981).
19. O. C. Jones, Jr., Flashing inception in flowing liquids. In *Non-equilibrium Two-phase Flow* (Edited by J. C. Chen and S. G. Bankoff), pp. 29–34. ASME, New York (1979).
20. J. M. Seynhaeve, M. M. Giot and A. A. Fritte, Non-equilibrium effects on critical flow rates at low qualities, CSNI Specialists Mtg on Transient Two-phase Flow, Toronto, 3–4 August (1976).
21. J. Riznic and M. Ishii, Modeling of vapor generation in flashing flow, ANL-86-1, NUREG/CR-4501, Argonne National Laboratory (December 1985).
22. A. R. Edwards, Conduction controlled flashing of a fluid and the prediction of critical flow rates in a one-dimensional system, AHSB Report (S), R-147 (1968).
23. M. S. Plesset and S. A. Zwick, The growth of vapor bubbles in superheated liquids, *J. Appl. Phys.* **25**(4) (April 1954).
24. H. K. Fauske, The discharge of saturated water through tubes, *Chem. Engng Prog. Symp. Ser.* **61**(59), 210–216 (1965). Paper presented at the 7th Natl Heat Transfer Conf., AIChE–ASME, Cleveland, Ohio, August (1984).
25. F. R. Zaloudek, Steam water critical flow from high pressure systems, NW 80535 (1964).

26. D. Malnes, Critical two-phase flow based on non-equilibrium effects. In *Non-equilibrium Two-phase Flows* (Edited by R. T. Lahey and G. B. Wallis). ASME, New York (1975).
27. U. S. Rohatgi and E. Reshotko, Non-equilibrium one-dimensional two-phase flow in variable area channels. In *Non-equilibrium Two-phase Flows* (Edited by R. T. Lahey and G. B. Wallis). ASME, New York (1975).
28. R. J. Simoneau, Pressure distribution in a converging–diverging nozzle during two-phase choked flow of subcooled nitrogen. In *Non-equilibrium Two-phase Flows* (Edited by R. T. Lahey and G. B. Wallis). ASME, New York (1975).
29. M. Studovic, Adiabatic vaporization in the superheated liquids, Ph.D. Thesis (in Serbo-Croatian), University of Belgrade (1982).
30. Md. Alamgir, C. Y. Kan and J. H. Lienhard, Early response of pressurized hot water in a pipe to a sudden break, EPRI NP-1867 (June 1981).
31. K. Wolfert, The simulation of blowdown processes with consideration thermodynamic phenomena, *Proc. CSNI Mtg on Transient Two-phase Flow*, Vol. 1, Toronto, 3–4 August (1976).
32. Y. A. Aleksandrov, G. S. Voronov, V. M. Gorbunkow, N. B. Delone and Y. I. Nechayev, *Bubble Chambers* (Translated by Scripta Technica, Inc.). Indiana University Press, Bloomington, Indiana (1962).
33. A. R. Edwards and T. P. O'Brien, Studies of phenomena connected with the depressurization of water reactors, *J. Brit. Nucl. Energy Soc.* **9**, 125–135 (1970).
34. P. Saha, Reactor safety research program, Quarterly Progress Report, BNL-NUREG-50683 (1972).
35. O. C. Jones, Jr. and T. S. Shin, Progress in modelling of flashing inception and critical discharge of initially subcooled liquids through nozzles, Joint Japan–U.S. Seminar on Two-phase Flow Dynamics, Lake Placid, New York, 29 July–3 August (1984).
36. T. S. Shin and O. C. Jones, Jr., A wall cavity model for flashing. Paper submitted for 23rd ASME/AIChE Natl Heat Transfer Conf., Denver, Colorado, 4–7 August (1985).
37. G. Kocamustafaogullari, I. Y. Chen and M. Ishii, Correlation for nucleation site density and its effect on interfacial area, NUREG/CR-2778, ANL-82-32, Argonne National Laboratory (May 1982).
38. M. Vomer, *Kinetik der Phasenbildung*. Steinhopf, Leipzig/Edward Bros., Ann Arbor (1945).
39. C. A. Ward, A. Balakrishnan and F. C. Hooper, On the thermodynamics of nucleation in weak gas–liquid solutions, *J. Basic Engng, ASME* **92**(4), 695–703 (December 1970).
40. T. W. Forest and C. A. Ward, Effect of a dissolved gas on the homogeneous nucleation pressure of a liquid, *J. Chem. Phys.* **66**(6), 2322–2330 (15 March 1977).
41. V. P. Skripov, *Metastable Liquids*. Wiley, New York (1974).
42. G. Kocamustafaogullari, Pressure dependence of bubble departure diameter for water, *Int. Commun. Heat Mass Transfer* **10**(6), 501–509 (November/December 1983).
43. N. Zuber, Nucleate boiling. The region of isolated bubbles and the similarity with natural convection, *Int. J. Heat Mass Transfer* **6**, 53–78 (1963).
44. J. Riznic, Non-equilibrium vapor generation in variable pressure fields (in Serbian), Ph.D. Thesis, Belgrade University (1987).
45. J. Joyce, ULYSSYS, Random House, New York (1962).
46. L. W. Florschuetz, C. L. Henry and A. R. Khan, Growth rates of free vapor bubbles in liquids at uniform superheats under normal and zero gravity conditions, *Int. J. Heat Mass Transfer* **12**, 1465–1489 (1969).

DENSITE NUMERIQUE DE BULLES ET FORMATION DE VAPEUR DANS L'ECOULEMENT AVEC DEPRESSURISATION

Résumé—Le phénomène de vaporisation relié à la décharge d'un liquide sous pression dans un environnement à basse pression est très important dans des systèmes industriels comme les réacteurs nucléaires et les réacteurs chimiques. Un nouveau modèle de ce mécanisme est proposé à partir de la théorie de la nucléation, du modèle de transport des bulles. Pour calculer la densité numérique des bulles, on utilise l'équation de transport avec une source distribuée sur des sites de nucléation à la paroi. Les prédictions du modèle en terme de fraction de vide sont comparés avec les données expérimentales Moby Dick et BNL. Au moins pour les conditions expérimentales considérées ici, la prédiction mécaniste du phénomène de vaporisation par détente est possible à partir du modèle de nucléation pariétale.

BLASENDICHTE UND DAMPFBILDUNG BEI DER ENTSPANNUNGSVERDAMPFUNG

Zusammenfassung—Das Phänomen der Entspannungsverdampfung beim plötzlichen Überströmen unterkühlter Flüssigkeit von einem hohen zu einem niederen Druckniveau ist für verschiedene industrielle Systeme wie Kernreaktoren und chemische Reaktoren sehr wichtig. Es wird ein neues Modell für die Entspannungsverdampfung vorgeschlagen, welches auf der Theorie der Blasenentstehung an einer Wand, einem Blasenwachstumsmodell und einem Drift-flux-Modell für die Blasenbewegung beruht. Zur Berechnung der Blasendichte wird die Transportgleichung für die Blasen mit einer verteilten Quelle für die Wandkeimstellen benutzt. Die Berechnungen des Dampfgehalts mit dem Modell werden mit experimentellen Daten von Moby Dick und BNL verglichen. Die Ergebnisse zeigen, daß—zumindest für die hier betrachteten experimentellen Bedingungen—die mechanistische Betrachtung der Entspannungsverdampfung möglich ist, die auf dem hier vorgestellten Modell für die Blasenbildung an einer Wand beruht.

ЧИСЛОВАЯ ПЛОТНОСТЬ ПУЗЫРЬКОВ И ПАРООБРАЗОВАНИЕ ПРИ ТЕЧЕНИИ ВСКИПАЮЩЕЙ ЖИДКОСТИ

Аннотация—Явление вскипания при истечении начально недогретой жидкости из сосуда высокого давления в среду с низким давлением часто встречается в таких промышленных системах, как например, атомные и химические реакторы. Предложена новая модель процесса вскипания, в основу которой положены теория зарождения пузырьков на стенке, модель роста пузырьков и модель их дрейфа. Для расчета числовой плотности пузырьков используется уравнение их переноса с распределенным источником зарождения на стенке. Результаты расчетов, представленные через объемные паросодержания, сравниваются с эксперимеитальными данными. Показано, что по крайней мере для рассматриваемых экспериментальных условий с помощью предлагаемой модели можно предсказать возникновение явления вскипания.